Supplemental Material

SIRT1 ameliorates lamin A/C deficiency-induced cardiac dysfunction by promoting mitochondrial bioenergetics

Running title: Lamin A/C-SIRT1 protects cardiac bioenergetics

Zunhui Du, M.S.[a,*], Yanting Zhou, M.S.[b,*], Qiheng Li, M.S.[a], Yuan Xie, M.S.[c], Tingfang Zhu, M.S.[a], Jing Qiao, M.S.[b], Ruihong Zhang, B.S.[b], Yangyang Bao, M.D., Ph.D.[a], Lingjie Wang, M.D., Ph.D.[a], Yinyin Xie, Ph.D.[b], Jinwei Quan, M.S.[a], Menglu Lin, M.S.[a], Ning Zhang, M.D., Ph.D.[a], Qi Jin, M.D., Ph.D.[a], Wenbin Liang, M.D., Ph.D.[d], Liqun Wu, M.D., Ph.D.[a], Tong Yin, M.D., Ph.D.[b,#] and Yucai Xie, M.D., Ph.D.[a,#]

[a] Department of Cardiovascular Medicine, Ruijin Hospital, Shanghai Jiao Tong University School of Medicine, Shanghai, China
[b] Shanghai Institute of Hematology, State Key Laboratory of Medical Genomics, National Research Center for Translational Medicine at Shanghai, Ruijin Hospital, Shanghai Jiao Tong University School of Medicine, Shanghai, China
[c] College of Osteopathic Medicine, Kansas City University, Kansas City, MO, United States
[d] University of Ottawa Heart Institute, Department of Cellular and Molecular Medicine, University of Ottawa, Canada
[*] These authors contributed equally to this work.

[#] Correspondence
Yucai Xie, Department of Cardiovascular Medicine, Ruijin Hospital, Shanghai Jiao Tong University School of Medicine. 197 Ruijin Second Road, Shanghai 200025, China. E-mail: xyc10530@rjh.com.cn;
Tong Yin, Shanghai Institute of Hematology, State Key Laboratory of Medical Genomics, National Research Center for Translational Medicine at Shanghai, Ruijin Hospital, Shanghai Jiao Tong University School of Medicine. 197 Ruijin Second Road, Shanghai 200025, China. E-mail: yt10961@rjh.com.cn;

Supplemental Methods

Untargeted proteomics

Sample preparation: Tissues were homogenized separately in 400 μL lysis buffer containing RIPA and Extraction Buffer, protease inhibitor, phosphatase inhibitor and 8 M urea using the gentleMACS Dissociator (Miltenyi Biotec). Extracted proteins were reduced and alkylated respectively with 10 mM dithiothreitol (Sigma-Aldrich, #D0632) and 15 mM iodoacetamide (Sangon Biotech, #A600539). Samples were precipitated with cold acetone at 1:5 volume ratio and centrifuged to retain the sediment, which was resuspended and digested with trypsin (Promega, #V5117/V5111) for 16 hours at 37℃ (1:50, enzyme-to-substrate). After desalted on SepPak C18 cartridges (Waters, #WAT036945), peptides were vacuum dried using Speed Vac.

LC-MS/MS: Digested peptides were first trapped on a precolumn (5 μm particle, 350 μm × 5 mm, ThermoFisher Scientific, #174500), and then separated on a C18 analytical column with an integrated CaptiveSpray Emmitter (1.6 μm particle, 250 mm × 75 μm, IonOpticks, #AUR2-25075C18A-CSI) on a nano Elute liquid chromatography (Bruker Daltonics). Buffer A and buffer B were 0.1% formic acid in water and 0.1% formic acid in acetonitrile, respectively. The column temperature was maintained at 50℃ and the gradient was 2%-22% B in 90 min, 22%-37% B in 10 min, 37%-80% B in 10 min, 80%-80% B in 10 min. The eluted peptides were then subjected to a timsTOF Pro (Bruker Daltonics) that operated in dia-PASEF mode. The dia-PASEF scheme contained 37 × 25 Th windows covering m/z from 375 to 1300 and 1/K0 from 0.6 to 1.6.

Database searching: Raw files were analyzed against the Mouse Swiss-Prot database (downloaded in January 2023, containing 17132 entries) with DIA-NN (version 1.8.1)[1] under library-free search with default settings. Briefly, Trypsin/P was protease with two maximum missed cleavages. Quantification strategy was Robust LC (high precision) with MBR enabled. The FDR cutoff at both precursor and protein level was 0.01. The proteome data generated can be viewed in integrated proteome resource iProX with IPX0006466000. Normalized data file is provided as Supplemental Table 1.

Proteomic data analysis: We identified a total of 6963 proteins in 22 samples. Proteome data were normalized via median centering and then log2 transformed. Proteins with > 40% missing values were excluded from downstream analysis. Differentially expressed proteins were filtered with fold change ≥ 1.3 and Student's t test p value ≤ 0.05. PCA plot was plotted via MetaboAnalyst (https://www.metaboanalyst.ca/). Gene set enrichment analysis (GSEA) was performed on WebGestalt (http://www.webgestalt.org/) to identify enriched KEGG and Reactome pathways. Heatmaps were generated with the R package 'ComplexHeatmap'.[2] Protein-protein interaction was analyzed on STRING and visualized via Cytoscape (version 3.9.1). Uniprot Keywords were further added to these interacting proteins by a Cytoscape plug-in stringApp with default settings.

Supplemental Table

Supplemental Table 1: 6240 quantified proteins in proteomics analysis

Supplemental Table 2: Table of RT-qPCR primer sequences

Gene	Species	Forward sequence (5′-3′)	Reverse sequence (5′-3′)
Nppa	Mouse	GAGAGACGGCAGTGCTTCTAGGC	CGTGACACACCACAAGGGCTTAGG
Nppb	Mouse	AGGCGAGACAAGGGAGAACA	GGAGATCCATGCCGCAGA
Myh7	Mouse	CGGACCTTGGAAGACCAGAT	GACAGCTCCCCATTCTCTGT
Col1a1	Mouse	GAGCGGAGAGTACTGGATCGA	CTGACCTGTCTCCATGTTGCA
Col3a1	Mouse	CTGTAACATGGAAACTGGGGAAA	CCATAGCTGAACTGAAAACCACC
Sirt1	Mouse	CAGCCGTCTCTGTGTCACAAA	GCACCGAGGAACTACCTGAT
Pgc1α	Mouse	TATGGAGTGACATAGAGTGTGCT	CCACTTCAATCCACCCAGAAAG
Tfam	Mouse	GGAATGTGGAGCGTGCTAAAA	ACAAGACTGATAGACGAGGGG
Nrf1	Mouse	AGCACGGAGTGACCCAAAC	TGTACGTGGCTACATGGACCT
Drp1	Mouse	TTACGGTTCCCTAAACTTCACG	GTCACGGGCAACCTTTTACGA

Fis1	Mouse	TGTCCAAGAGCACGCAATTTG	CCTCGCACATACTTTAGAGCCTT
Mff	Mouse	ATGCCAGTGTGATAATGCAAGT	CTCGGCTCTCTTCGCTTTG
Mfn1	Mouse	CCTACTGCTCCTTCTAACCCA	AGGGACGCCAATCCTGTGA
Mfn2	Mouse	AGAACTGGACCCGGTTACCA	CACTTCGCTGATACCCCTGA
Prkn	Mouse	GGTCCTACAGACAGGGCAATA	CTGGCCTTTCCTCACACCAC
Pink1	Mouse	TTCTTCCGCCAGTCGGTAG	CTGCTTCTCCTCGATCAGCC
Gapdh	Mouse	AGGTCGGTGTGAACGGATTTG	TGTAGACCATGTAGTTGAGGTCA
18sRNA	Mouse	GGACAGGATTGACAGATTGATAG	ATCGCTCCACCAACTAAGAA

Supplemental References

1. Demichev V, Messner CB, Vernardis SI, Lilley KS, Ralser M. DIA-NN: neural networks and interference correction enable deep proteome coverage in high throughput. Nat Methods 2020;17:41-44.
2. Gu Z, Eils R, Schlesner M. Complex heatmaps reveal patterns and correlations

in multidimensional genomic data. Bioinformatics 2016;32:2847-9.

Supplemental figure and legends

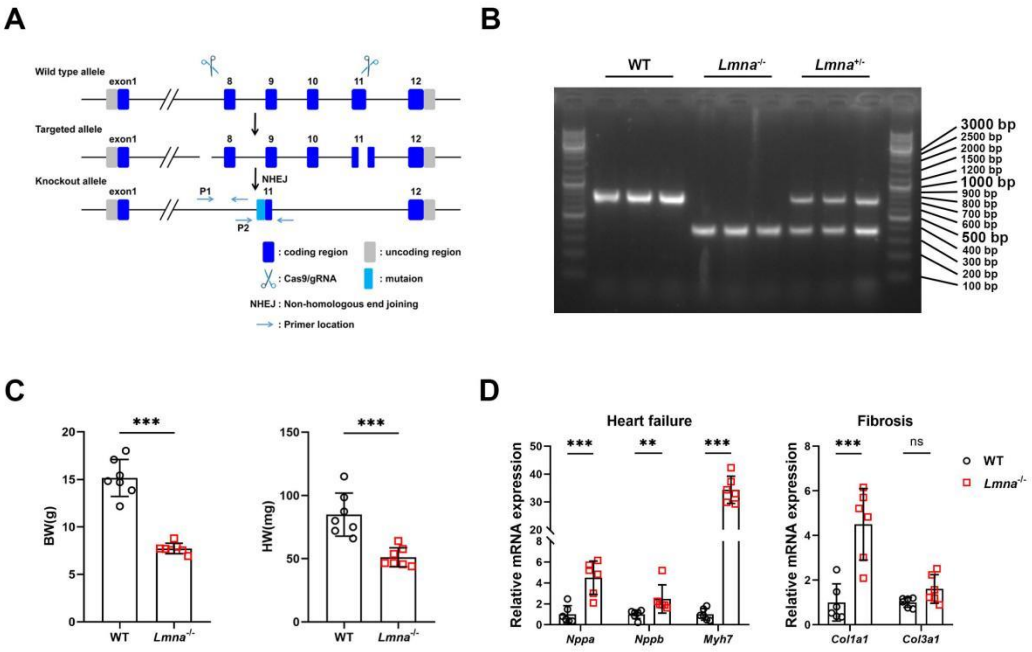

Supplemental Figure 1. 1-month-old *Lmna*$^{-/-}$ mice show decreased body and heart weight, increased markers of heart failure and fibrosis.

A. Design diagram showing knockout of *LMNA* exons 8-11 through non-homologous recombination repair introducing mutation using CRISPR/Cas9 technique. **B**. PCR analysis of WT, *Lmna*$^{-/-}$ and *Lmna*$^{+/-}$ mice. A 679 bp fragment was observed in WT mice, a 353 bp fragment was observed in *Lmna*$^{-/-}$ mice, and both fragments were observed in *Lmna*$^{+/-}$ mice. **C**. Heart weight (HW), body weight (BW) of 1-month-old WT and *Lmna*$^{-/-}$ mice (n=7). **D**. qPCR quantitative analysis of genes related to heart failure (*Nppa*, *Nppb*, *Myh7*) and fibrosis (*Col1a1*, *Col3a1*) in 1-month-old WT and *Lmna*$^{-/-}$ hearts (n=6). Data are presented as mean ± SD and compared by t-test in figures **C**, **D** (*nppa*,

myh7, *col1a1*, *col3a1*) or by Mann-Whitney U test in **D** (*nppb*). $^{**}P < 0.01$, $^{***}P < 0.001$.

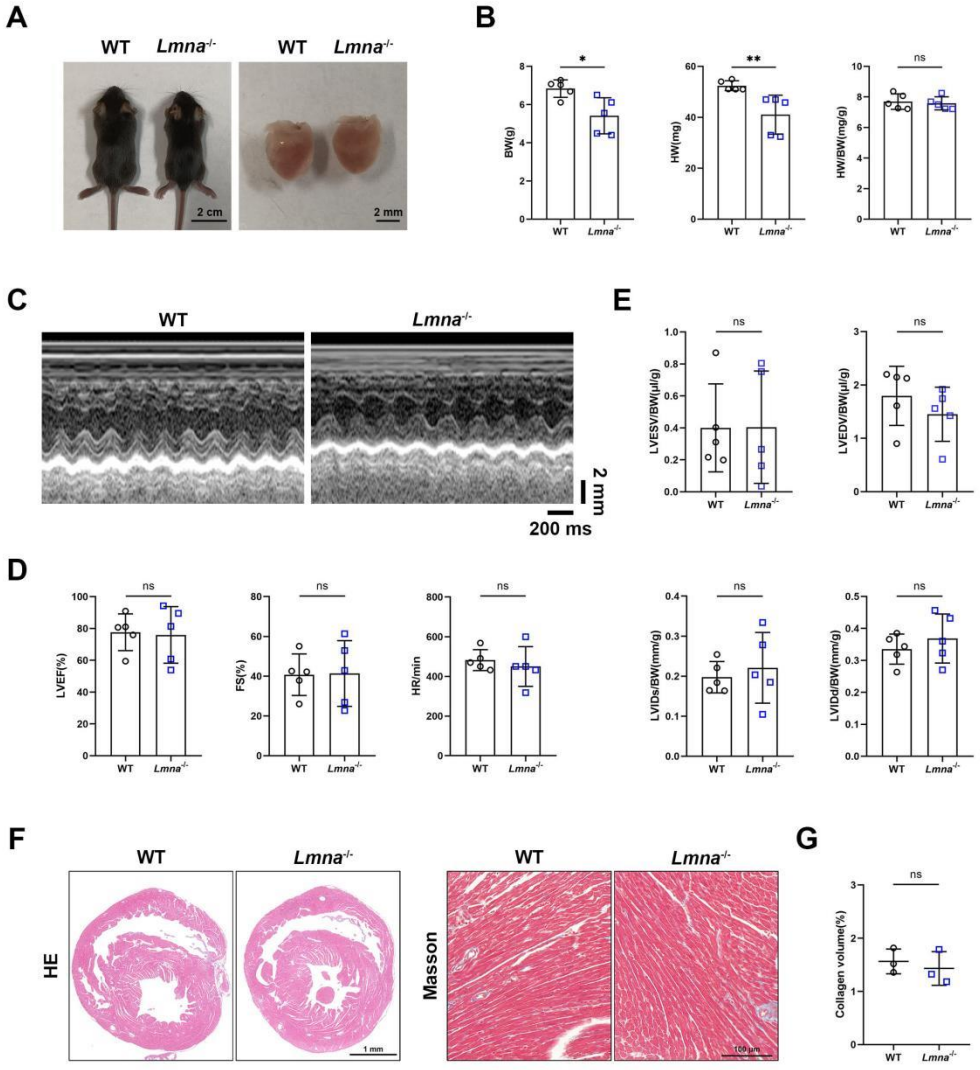

Supplemental Figure 2. 2-week-old *Lmna*$^{-/-}$ mice show no significant DCM phenotype.

A. Representative exteriors (scale bar: 2 cm) and cardiac appearances (scale bar: 2 mm) of 2-week-old WT and *Lmna*$^{-/-}$ mice. **B**. Heart weight (HW), body weight (BW), HW/BW of WT and *Lmna*$^{-/-}$ mice (n=5). **C**. Representative echocardiography of WT

and *Lmna*$^{-/-}$ mice. **D**. Left ventricular ejection fraction (LVEF), shortening fraction (FS) and heart rate (HR) in WT and *Lmna*$^{-/-}$ mice (n=7). **E**. Left ventricular end-systolic volume (LVESV)/BW, left ventricular end-diastolic volume (LVEDV)/BW, left ventricular end-systolic diameter (LVIDs)/BW, left ventricular end-diastolic diameter (LVIDd)/BW in WT and *Lmna*$^{-/-}$ mice (n=5). **F**. Representative HE staining (scale bar: 1 mm) and Masson Trichrome staining (scale bar: 100 μm) images of the ventricular transverse section of WT and *Lmna*$^{-/-}$ mice. **G**. Quantification of the percentage of collagen in myocardial tissue of WT and *Lmna*$^{-/-}$ mice (n=3). Data are presented as mean ± SD and compared by t-test in figures **B** (BW, HW/BW), **D**, **E,** and **G** or by Mann-Whitney U test in **B** (HW). **P* < 0.05, ***P* < 0.01, ns: no significant difference.

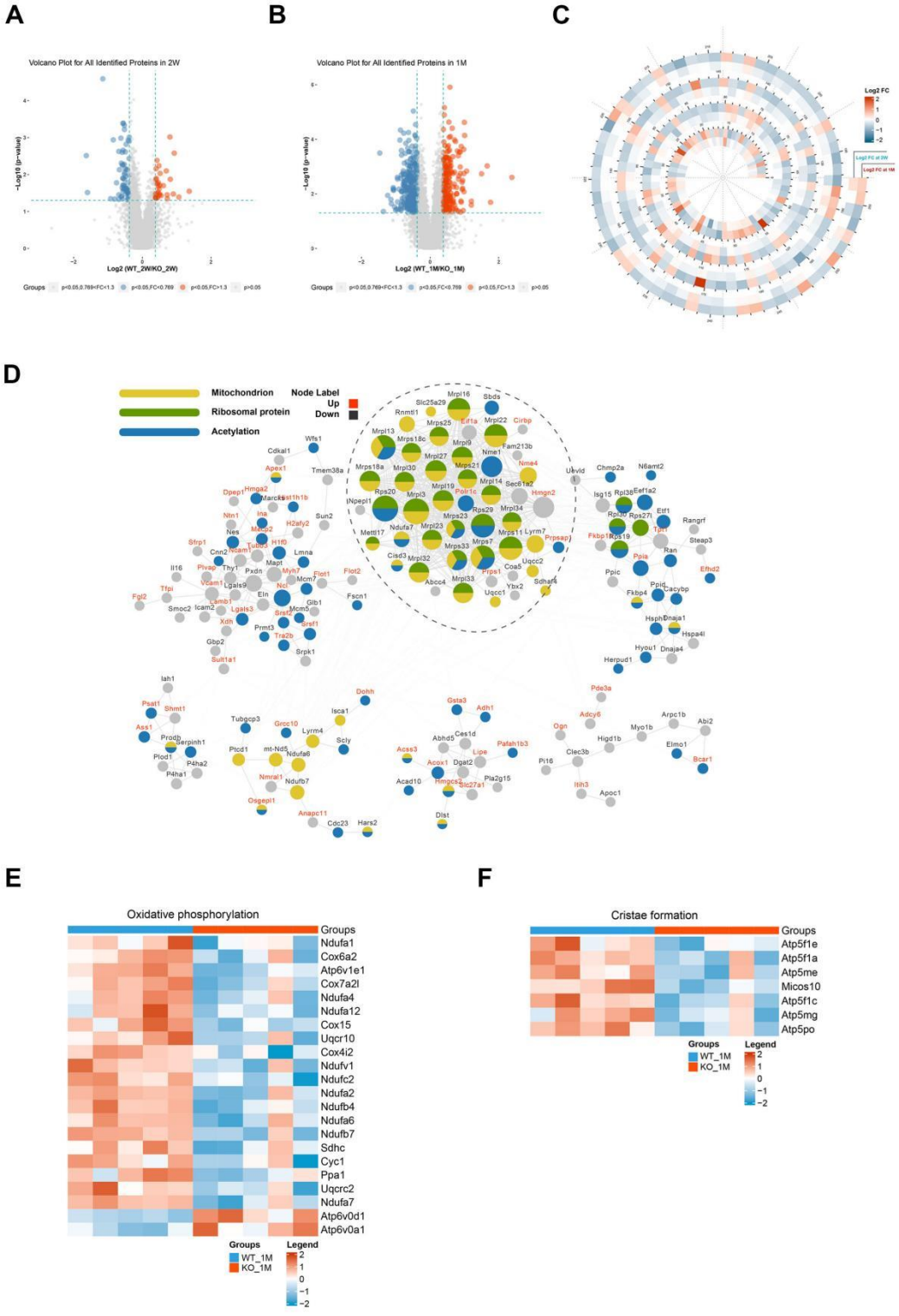

Supplemental Figure 3. Volcano blot, networks analysis and hierarchical clustering.

A-B. Volcano blot of all proteins detected in 2-week (A) and 1-month-old (B) WT and

Lmna$^{-/-}$ mice. **C**. Spiral plot summarizing 257 consistently changed differentially expressed proteins (DEPs) in 1-month and 2-week-old WT and *Lmna*$^{-/-}$ mice. **D**. Protein-Protein Interaction (PPI) networks analysis illustrating functional protein nodes. Node colors represent different Uniprot Keywords. Node label colors represent up and down-regulated DEPs. **E**. Heatmap summarizing differential expressed oxidative phosphorylation proteins in 1-month-old WT and *Lmna*$^{-/-}$ mice. **F**. Heatmap summarizing differential expressed cristae formation proteins in 1-month-old WT and *Lmna*$^{-/-}$ hearts.

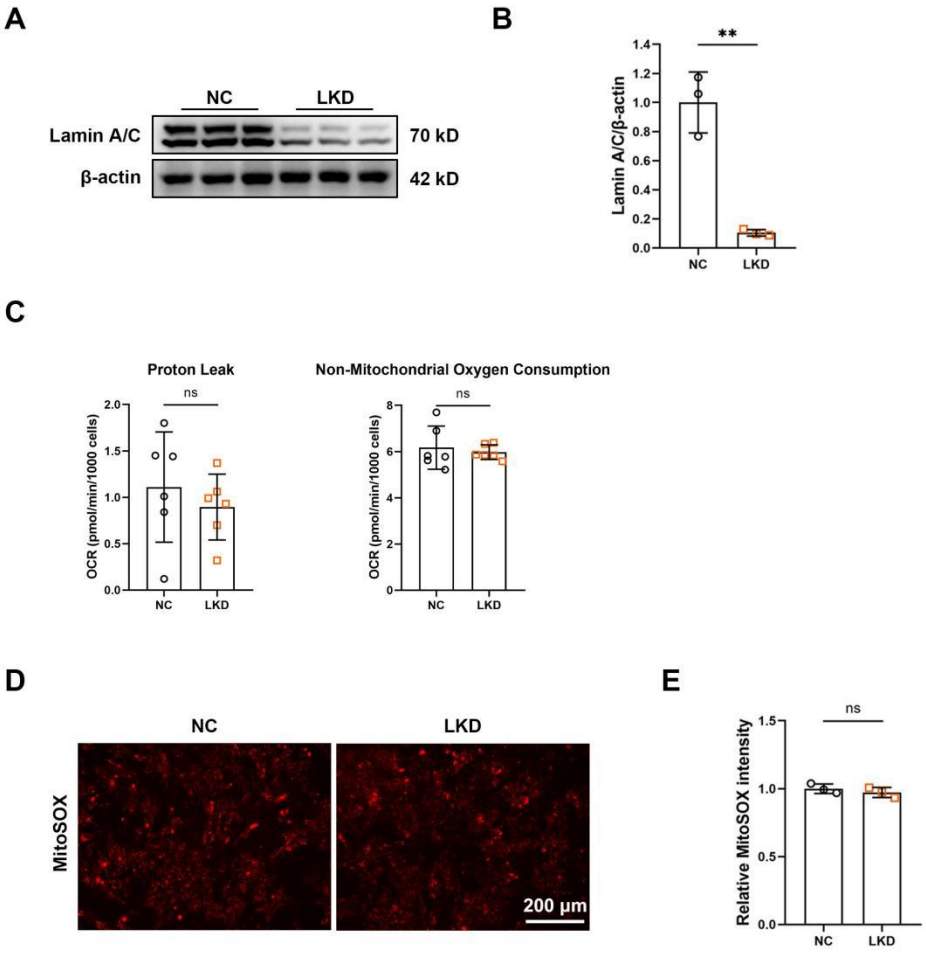

Supplemental Figure 4. Lamin A/C knockdown leads to aberrant oxidative

respiration capacity.

A. Representative WB images of lamin A/C in NC and LKD NRVMs. **B**. Quantification of lamin A/C level normalized to β-actin (n=3). **C**. Quantification of proton leak, non-mitochondrial oxygen consumption in NC and LKD NRVMs (n=6). **D**. Representative fluorescence images showing mitochondrial superoxide in NC (negative control) and lamin A/C knockdown (LKD) neonatal rat ventricular myocytes (NRVMs) stained by MitoSOX. Scale bar: 200 μm. **E**. Quantification of MitoSOX intensity (n=3). Data are presented as mean ± SD and compared using t-test in figures **B**, **C**, and **E** by two-tailed t test. $^{**}P < 0.01$, ns: no significant difference.

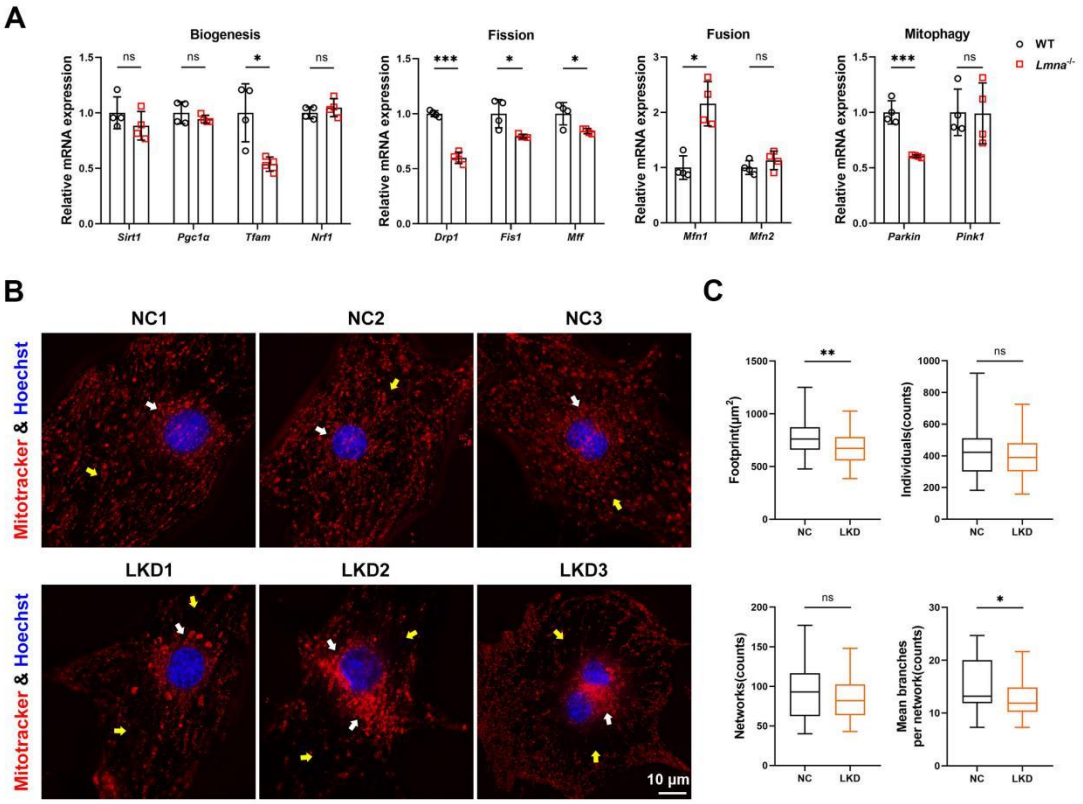

Supplemental Figure 5. Lamin A/C deficiency causes abnormal expression of

genes related to MQC and aberrant mitochondrial morphology.

A. qPCR quantification of genes related to mitochondrial biogenesis (*Sirt1*, *Pgc1α*, *Tfam*, *Nrf1*), fission (*Drp1*, *Fis1*, *Mff*), fusion (*Mfn1*, *Mfn2*) and mitophagy (*Parkin*, *Pink1*) in 1-month-old WT and $Lmna^{-/-}$ hearts (n=4). **B**. Representative 3 pairs of fluorescence images showing mitochondrial morphology of NC and LKD NRVMs stained by Mitotracker (red) and Hoechst (blue). White arrows denote perinuclear mitochondria. Yellow arrows denote intermyofibrillar mitochondria. Scale bar: 10 μm. **C**. Mitochondrial network quantitative analysis of mitochondrial footprint, individuals, networks, mean branches per network in NC and LKD NRVMs (NC, n=30; LKD, n=37). Data are presented as mean ± SD and compared using t-test in figures **A**, **C** (footprint, individuals, networks) or Mann-Whitney U in figure **C** (mean branches per network). $*P < 0.05$, $**P < 0.01$, $***P < 0.001$, ns: no significant difference. Abbreviations as in Supplemental figure 4.

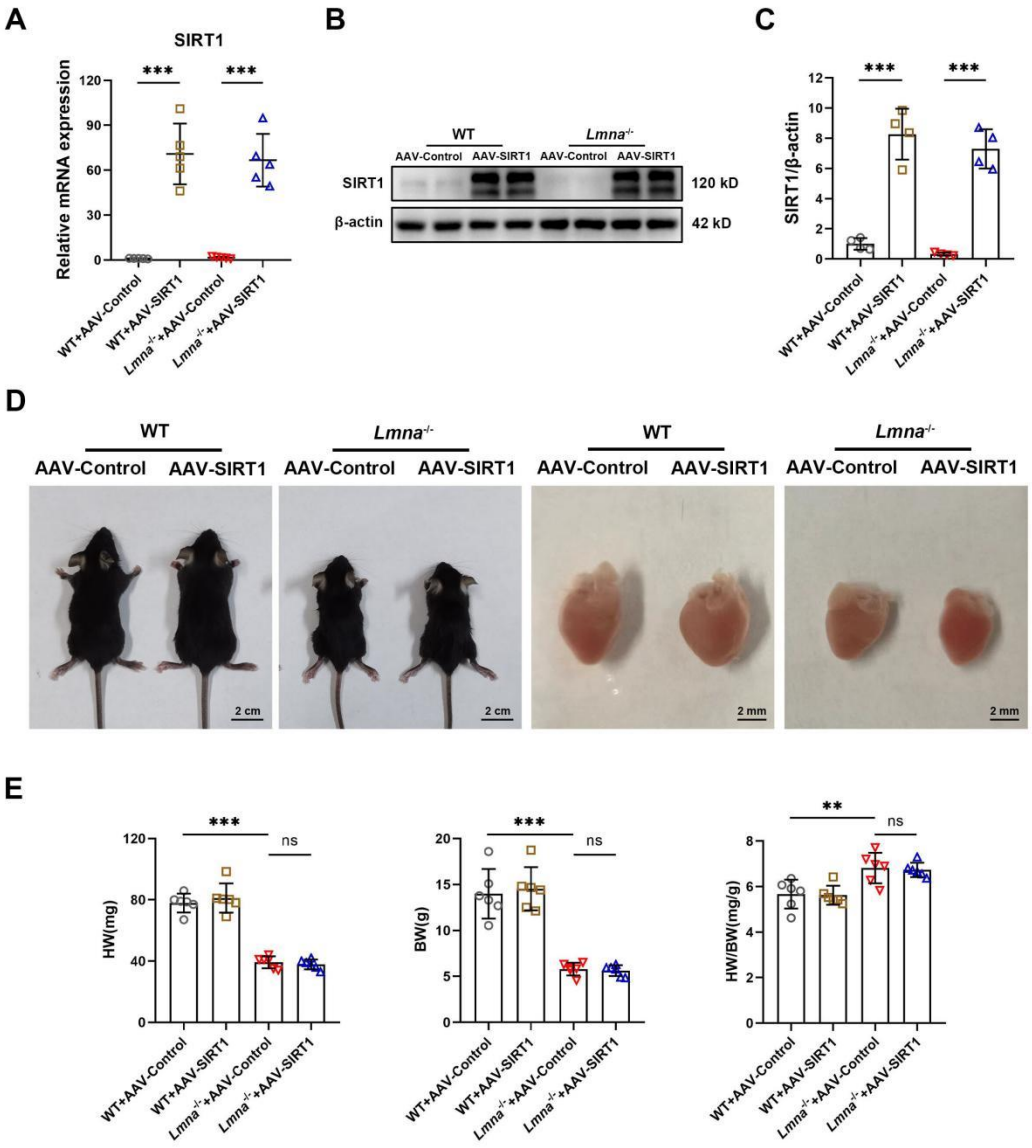

Supplemental Figure 6. AAV-SIRT1 injection results no improvement in exteriors, BW, HW, or HW/BW of *Lmna*$^{-/-}$ mice.

A. qPCR quantitative analysis of sirt1 mRNA level in WT and *Lmna*$^{-/-}$ mice hearts pre-treated with AAV-CMV-SIRT1-mNeonGreen (AAV-SIRT1) or AAV-CMV-mNeonGreen (AAV-Control) (n=5). **B**. Representative WB images of SIRT1 in 1-month WT and *Lmna*$^{-/-}$ hearts pre-treated with AAV-SIRT1 or AAV-Control. **C**. Quantification of SIRT1 expression level normalized to β-actin (n=4). **D**.

Representative exteriors (scale bar: 2 cm) and cardiac appearances (scale bar: 2 mm) of WT and *Lmna*$^{-/-}$ mice pre-treated with AAV-SIRT1 or AAV-Control. **E**. Heart weight (HW), body weight (BW), HW/BW of WT and *Lmna*$^{-/-}$ mice pre-treated with AAV-SIRT1 or AAV-Control (n=6). Data are presented as mean ± SD and compared using ANOVA with Tukey post-hoc test in figures **A**, **C**, and **E**. $^{**}P < 0.01$, $^{***}P < 0.001$, ns: no significant difference.